А С Т Р О Ф И З И К А

ТОМ 60 ФЕВРАЛЬ, 2017 ВЫПУСК 1

THE EFFECTS OF VISCOSITY IH THE SHOCK WAVES OBSERVED AFTER TWO DIFFERENT CORONAL MASS EJECTION ACTIVITIES CME20/11/2003 AND CME11/04/2010

H.CAVUS[1], G.ZEYBEK[2]

Received 16 April 2016
Accepted 14 December 2016

Coronal mass ejections are main results of the powerful solar activity. These activities are capable of generating shock waves in the interplanetary medium. The shock waves happen when the solar particles change their velocities from the supersonic to the subsonic nature. Since, the interaction of shock waves with viscosity is one of the central problems in the supersonic regime of compressible gas flow, the investigations of these events play a crucial role in space weather purposes [1]. The main purpose of this study is to search the effects of viscosity on the shock waves observed after the CMEs of 20/11/2003 and CME11/04/2010.

Key words: *Shock waves: Viscosity: Reynolds number: Coronal mass ejection*

1. *Introduction*. The corona is the outermost level of the solar atmosphere. It is located above the chromospheric layer. The temperature rate of coronal jumps suddenly changes from a few thousands to a few millions Kelvins [2]. Various features including plumes, loops and streamers happen in the corona. These phenomena have attracted the space physicists due to their complex structures. Physical activities of the corona and their natures are known to be directly affected by the solar sunspot cycle [3].

The magnetic plasma structures in the solar corona are rather complex. There are two main structures called "magnetically closed" and "magnetically open" structures. The magnetic field and plasma interaction characterize the type of phenomena [3]. A transient CME occurred by producing an enormous plasma cloud in the interplanetary space due to the expansion of closed magnetic loop structures [4]. Sometimes a stream of plasma expands into the interplanetary space from coronal holes as a result of magnetically open structures [5]. At the level of coronal temperatures, the plasma stream is no longer bound to the Sun. It may expand into the interplanetary medium at some supersonic speeds, defined as the solar wind. Recently, plumes observed outside of the coronal holes have been suggested as other possible sources of the solar wind [6].

Because of interactions with the local interplanetary medium, the supersonic motions of the particles ejected from the Sun may cause a shock wave. There are many ways to generate shocks due to solar particles such as CMEs, blast waves and fast streams emitted from the Sun [7]. They, of course, can cause some physical phenomena such as compression, heating, and a change in the magnetic field.

The solar wind was first defined as a continuous outpouring of particles generated from the Sun. As the high-speed solar wind moves into the interplanetary medium, it can produce a shock wave. The Kelvin-Helmholtz instability of the solar atmosphere was studied in [8]. The authors found that the range of radial velocity is 380 km/s for slow and 780 km/s for fast solar winds. The shock wave arises, since solar wind particles are emitted at these velocities [9], while the speed of sound is about 100 km/s [10,11]. These shocks were observed through an observation project SOHO/LASCO and published in [12]. They showed that the shocks can be detected at least for some cases of CMEs and solar winds. The ejected solar particles travelling faster than the solar speed will drive a shock ahead and produce a decreasing speed profile within the ejecta [13]. These shock features can be deduced from the associated compression of density [14].

A little portion of shock wave studies have concentrated on the complicated subject of entropy change. For example, [15] considered the entropy distribution across the shock layer without viscosity and the heat conduction. In their study, the entropy increases up to its maximum at the centre of the shock front and then it decreases in the other half of the front. This does not violate the second law of thermodynamics, since this law is valid for the entire of the system. Similarly, the authors of [16] worked on the change of entropy across the shocks in an ordinary dusty gas by means of Navier-Stokes equations where they show that the entropy profile has its maximum within the shock front. Besides this result it is also demonstrated that the entropy increases across the shock wave with the Mach number of upstream and density of particles. Others concentrated on the attitude of the entropy in the shock wave occurring in the interplanetary medium after CME12/12/2006 [17] by applying the model of [18].

The project of NASA-ACE detects these events routinely. The papers [19,20] studied the shocks that happened after the CMEs of November 20, 2003 and April 11, 2010 by the use of NASA-ACE data. In the present paper, the model presented in the studies of [17,18,21] will be applied to the shocks appearing after these CMEs.

The model predicting the arrival of shock waves to the Earth was made in [22]. Unlike this work, the main goal of this study is to search the effects of viscosity for the shocks that occurred after these two CMEs given in the last paragraph. To complete the modelling of such shocks, the Navier-Stokes equations are to be solved with the use of our model (e.g. [18]). Mathematically this study can be approximated to the hydrodynamic case as given in the section 2. In this process, the behaviour of a gas including viscosity can be expressed in terms of Reynolds number [23], as in [18] and [24]. In section 3, the physical properties of the downstream of the shocks happening after CMEs of November 20, 2003 (hereafter CME20/11/2003) and April 11, 2010 (hereafter CME11/04/2010) will be shown. In section 4, the results are compared with those in similar works.

2. *Physical formulation of the problem.*

2.1. *Basic physical properties of the problem.* The physical structure of the solar atmosphere is a complex plasma in which the magnetic and gas pressures play important interchanging roles with respect to their dominances. This dominancy is determined by the plasma-β (the ratio of gas pressure to magnetic pressure). The gas pressure of plasma dominates if $\beta > 1$, and if $\beta < 1$, the magnetic pressure of plasma becomes dominant.

The plasma-β has greater values ($\beta >> 1$) in the acceleration region of the solar wind, which is theoretically defined as infinity [25]. The value used in the model of [26] is 44 and changes to infinity. Therefore, one can easily deduce that the gas portion of pressure plays an important role in the dynamics of the solar wind [27].

The duration of CME is determined by combining the profiles of density, temperature and velocity. We use two different shock waves that occurred after CME20/11/2003 and CME11/04/2010. The values of upstream parameters can be obtained from ACE mission, given in Table 1 [19,20]. The aim of the present work is to demonstrate the effects of viscosity in the shock waves observed after these CMEs by using the model given in [18]. The parameters listed in Table 1 are used for the present analysis.

Table 1

UPSTREAM PHYSICAL PARAMETERS FOR SHOCK WAVES, GIVEN IN [19,20]

	n_1 (cm^{-3})	T_1 (Kelvins)	u_1 (km/s)
CME20/11/2003	6.23	3.63×10^4	438
CME11/04/2010	1.8	3.98×10^4	373

In many cases, CME can be detected from the behaviour of the density data, which give an information about the occurrence of shock [22]. As shown in Table 1, the velocities were given as 438 km/s and 373 km/s for CME20/11/2003 and CME11/04/2010 respectively. As it was mentioned above, the local sound speed is about 100 km/s in the interplanetary medium, indicating that, the shock wave came to existence. The upstream temperatures of these shock waves were about 3.63×10^4 K and 3.98×10^4 K, respectively for the CME20/11/2003 and CME11/04/2010 shocks (Table 1).

2.2. ***Basic formulation***. The plasma β

$$\beta=\frac{p_{gas}}{p_{mag}} \tag{1}$$

has higher values in the solar wind [25-28] indicating that, the gas pressure plays a more crucial role than the magnetic one. Therefore, the solar wind can be driven by gas part pressure at coronal temperatures. The problem can be transformed to the hydrodynamic problem as in [29-30] in which the basic theories of solar and stellar winds can be found.

For the case of a compressible and viscous shock in steady flow, a fundamental equation is obtained in [18]

$$\left[\left(\frac{1}{2}-\frac{4}{3}\frac{1}{Re_1}\right)(\gamma-1)M_1^2+1\right]\kappa^2-\left[\left(1-\frac{4}{3}\frac{1}{Re_1}\right)\gamma M_1^2+1\right]\kappa+\left(\frac{\gamma+1}{2}-\frac{4}{3}\frac{1}{Re_2}\right)M_1^2=0. \tag{2}$$

The subscripts 1 and 2 show the up and downstream of the shock respectively. In the last equation, Re_1 and Re_2 are the values of Reynolds number. The quantities γ, κ and M_1 are the adiabatic index (i.e. the ratio of specific heats), compression rate (a ratio of downstream density to upstream density) and the upstream value of Mach number, respectively. The values of M_1, Re_1 and Re_2 in Eq. (2) affect the distributions of physical parameters in the downstream of the shock. The value of γ satisfies the relation $5/3<\gamma<3$ for a collisionless shock front, and were used in [31,32] to find the downstream physical parameters. The entropy change (S_2 - S_1) can be found by the use of [17]:

$$S_2-S_1=c_V\ln\left[\frac{p_2}{p_1}\kappa^{-\gamma}\right] \tag{3}$$

2.3. ***Value of the downstream Reynolds number in the solar wind***. Reynolds number has great importance in the dynamics of the interplanetary region. It takes values between 10^{12} and 10^{14} in the solar wind acceleration region ([6,33]).

In order to solve the problem, Re_2 can be expressed as a function of γ, Re_1 and M_1 similar to the works of [18] and [24]. The ratio Re_2/Re_1 is shown as a function of M_1 in the left part of Fig.1. It has a diminishing tendency with the increasing values of M_1. As M_1 increases and Re_2/Re_1 is equal to unity (i.e. $Re_1=Re_2$) for the value of M_1 is about 2. This value corresponds to a transition regime changing from weak to strong shocks (i.e. for weak shocks $M_1<2$ and for strong shocks $M_1>2$) [18,34,35].

The change of Re_2 with respect to Re_1 for different values of M_1 is demonstrated in the right side of Fig.1 for a monatomic gas of $\gamma = 5/3$ [21] and [35]. It increases with respect to increasing values of Re_1. Another important result seen from this plot is that, Re_2 has larger values for smaller values of M_1.

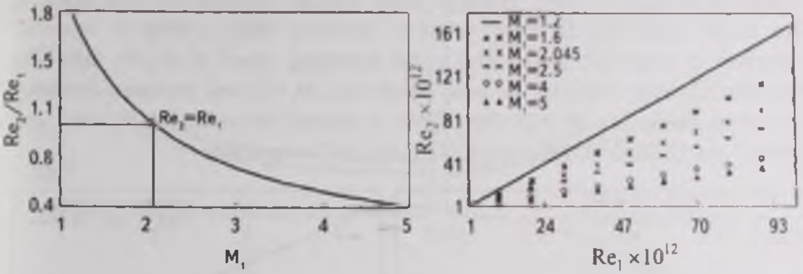

Fig.1. Upstream dependencies of downstream Reynolds number (Re_2) with respect to M_1 (left) and Re_1 (right) [21].

3. *Model Results for the Shock Wave Produced after the CME18/02/1999 and CME28/04/2001.* Downstream values in the shocks produced by the CME20/11/2003 and CME11/04/2010 were found from some solutions of equations (2-3). The method was adapted to Maple 9.5. Results for the downstream values of some physical parameters are represented in Table 2 and in Fig.2-8). In these calculations, the value of Re_1 is taken to be 10^{13} [6].

In Table 2 the variations of some parameters are presented, in which, physical structure of the problem is described for different values of the upstream Mach number. These parameters are Re_2/Re_1, κ (i.e. n_2/n_1), u_2/u_1, T_2/T_1, S_2-S_1 and M_2/M_1. The critical value of M_1 for the turning point was found as $M_1 = 2.045$ at which Re_2/Re_1 is equal to unity as given in Fig.1. This point is not only important for Re_2/Re_1 but also for the strength of shocks [18]. Re_2/Re_1, u_2/u_1 and M_2/M_1 have decreasing trends with increasing values of M_1. These decreasing trends in these parameters slow down after the critical value $M_1 = 2.045$. κ, T_2/T_1 and $S_2 - S_1$ have

Table 2

DISTRIBUTIONS OF SOME PHYSICAL PARAMETERS FOR DIFFERENT VALUES OF M_1

M_1	Re_2/Re_1	n_2/n_1	u_2/u_1	T_2/T_1	$S_2 - S_1$	M_2/M_1
1.200	1.704	1.297	0.771	1.195	0.055	0.705
1.600	1.278	1.842	0.543	1.602	0.798	0.429
2.045	1.000	3.329	0.437	2.137	2.441	0.294
2.500	0.818	2.703	0.370	2.798	4.566	0.221
4.000	0.511	3.368	0.297	5.863	11.961	0.123
5.000	0.409	3.571	0.280	8.680	16.368	0.095

both increasing tendencies with the increasing M_1. This tendency slows down for n_2/n_1 speeds up for T_2/T_1 and $S_2 - S_1$ after $M_1 = 2.045$.

Fig.2 demonstrates the dependencies of n_2 with respect to M_1 (left) and Re_2/Re_1 (right) by the use of density values in Table 1 as an upstream for both cases. n_2 has greater values for the higher values of upstream Mach number as expected. However, it is inversely proportional to the increasing values of Re_2/Re_1 [18]. The variation has linear tendency for weak shocks (i.e. $M_1 < 2$) and nonlinear tendency for strong shocks (i.e. $M_1 > 2$). For $M_1 = 5$, it reaches the values of $22.3\,cm^{-3}$ and $6.4\,cm^{-3}$ for CME20/11/2003 and CME11/04/2010 respectively.

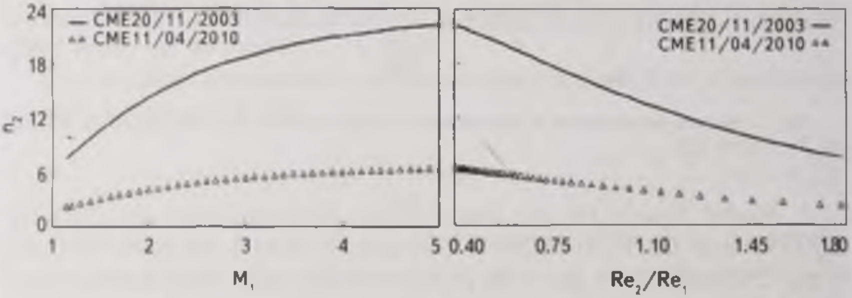

Fig.2. Variation of downstream density (in cm^{-3}) with respect to M_1 (left) and Re_2/Re_1 (right) for both CME20/11/2003 and CME11/04/2010.

The Fig.3 shows the changes of T_2 with M_1 and Re_2/Re_1. For weak shocks, the variations are small compared with the variations for strong shocks. The values of 3.63×10^4 and 3.98×10^4 K are used as T_1 in Table 1. As also shown in Table 2, for weak shocks there are small changes in the values of T_2. However, the changes are big for strong shocks. It reaches the values of 3.15×10^5 K and 3.45×10^5 K with the higher values M_1 for CME20/11/2003 and CME11/04/2010.

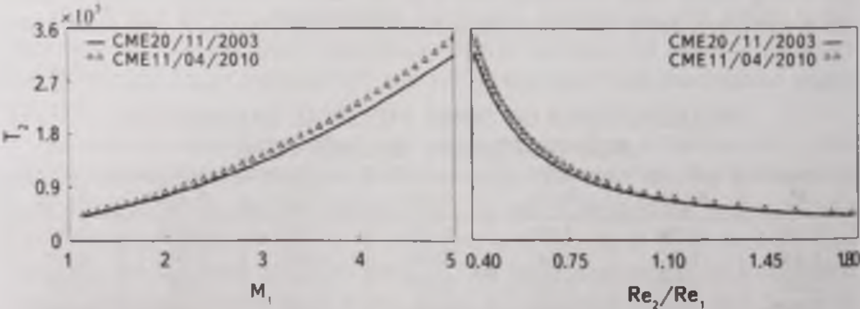

Fig.3. Dependencies of T_2 (in Kelvins) with respect to M_1 and Re_2/Re_1 values for both CME20/11/2003 and CME11/04/2010.

Fig.4 gives the variations of u_2 with respect to M_1 and Re_2/Re_1. Their u_1 values are taken from Table 1 for both CMEs. Unlike the T_2, for $M_1 < 2$ the changes in u_2 are large compared with the variations for $M_1 > 2$.

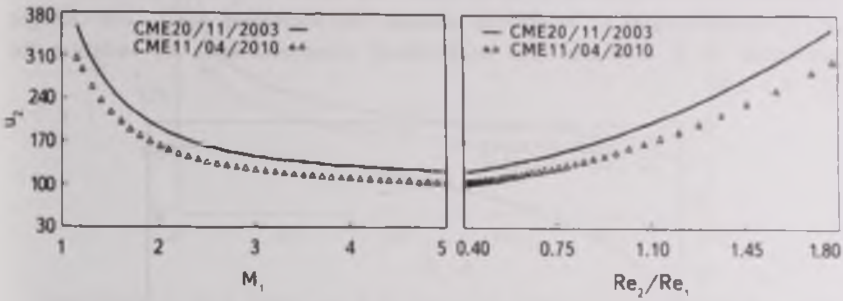

Fig.4. Behaviours of u_2 as a function of M_1 and Re_2/Re_1 values.

Fig.5 shows the changes of Re_2/Re_1, n_2/n_1, u_2/u_1 and T_2/T_1 with respect to $S_2 - S_1$. T_2/T_1 shown as cross symbols has an increasing behaviour with increasing values of entropy difference. n_2/n_1 represented as empty squares also has an increasing behaviour for increasing values of $S_2 - S_1$ similar to temperature ratio. However, the Re_2/Re_1 shown as empty triangles have decreasing tendency. The u_2/u_1 given as plus signs is also in decreasing trend for increasing $S_2 - S_1$. All of these ratios are unity for the isentropic case (i.e. $S_2 - S_1 = 0$). In other words, no shock happens for $S_2 - S_1 = 0$ since $\kappa = 1$ (i.e. no compression).

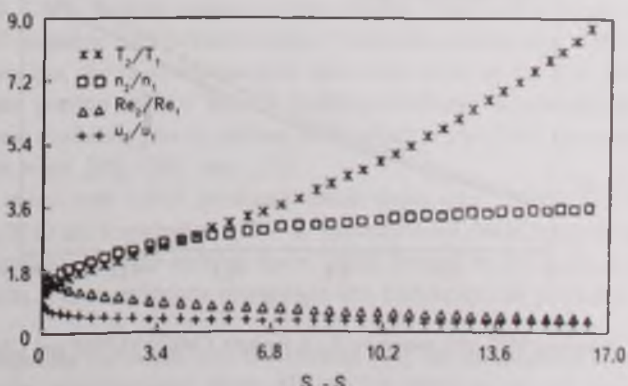

Fig.5. Variations of some parameters with respect to $S_2 - S_1$.

The variation n_2 is presented in Fig.6 for $S_2 - S_1$. $S_2 - S_1 < 2.44$ (i.e. $M_1 \leq 2$) which can be defined as a weak shock as shown in Table 2. The downstream density has greater values for the higher values of $S_2 - S_1$ as expected. For small values of entropy difference $S_2 - S_1$ there are big changes in the values of n_2. However, the variations are small for increasing values of $S_2 - S_1$. Fig.7 depicts the $S_2 - S_1$ dependency of T_2. It tends to increase with increasing $S_2 - S_1$. The changes are small for $S_2 - S_1 < 2.44$ (i.e. weak shock) compared with the variation for $S_2 - S_1 > 2.44$.

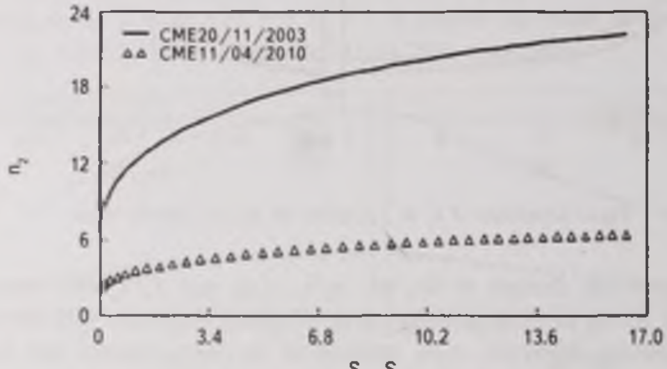

Fig.6. Changes of downstream density with respect to $S_2 - S_1$ for both CME20/11/2003 and CME11/04/2010.

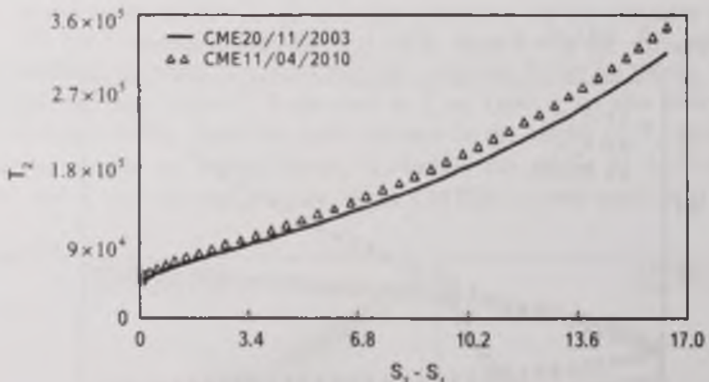

Fig.7. Variations of T_2 with respect to $S_2 - S_1$ for both CME20/11/2003 and CME11/04/2010.

The variation of u_2 given in Fig.8 is decreasing for higher values of $S_2 - S_1$, as expected. The changes in downstream velocity are small for higher values of the entropy difference. The very weak shocks are nearly isentropic i.e. S_2 is very close to its upstream value (see Table 2). On the other hand, the change is high for strong shocks ($M_1 >> 2$).

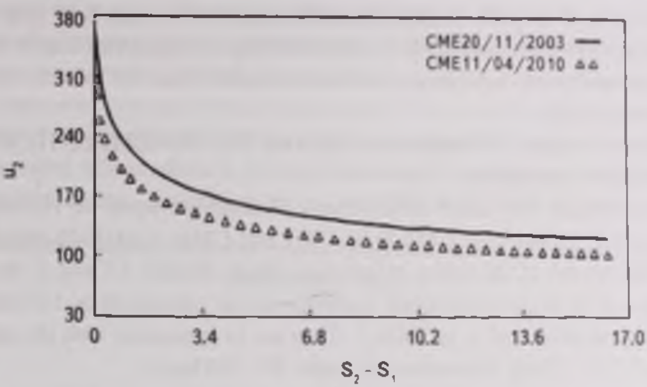

Fig.8. Variations of T_2 with respect to $S_2 - S_1$ for both CME18/02/1999 and CME28/04/2001.

4. ***Discussion and Conclusion***. CMEs and solar wind are two main activities of the Sun producing shocks and geomagnetic storms. Therefore, the study of such activities is very important for space physics. In other words, the study of CME driven shocks in interplanetary space is one of the most important issues for space weather purposes. Enough amount of energy can be released rapidly from the Sun to produce a CME to drive a shock in interplanetary medium [13]. Understanding the evolution of the physical parameters remains still a very complicated subject limited by observational capabilities.

When a CME activity occurs in the corona, there are complex physical processes of magnetic and thermal energy. During the interactions in the ambient interplanetary gas, the magnetic pressure dominates closer to the Sun. Far beyond the Sun gas portion of the plasma pressure becomes dominant. Therefore, hydrodynamic modelling can be applied to the study of the CME produced shocks in the solar wind [25], [26] and [27].

In this study, two CME produced shock waves after CME20/11/2003 and CME11/04/2010 are investigated and 1 - D hydrodynamic model analysis was made for shock propagation in the ambient space, which focused on the study of Reynolds number effects. The conclusions obtained in this manuscript are presented item by item:

- Comparing our result with the work of [19], the downstream value of the plasma density approximately about $22.5\,\mathrm{cm}^{-3}$ is fitted to $M_1 \approx 5$ case in this present model (given in Fig.2). In the work of [20] the downstream value of density is given as about $5.8\,\mathrm{cm}^{-3}$. This result corresponds to the case of $M_1 \approx 3.6$ in our model. These results are in good accordance with shock waves of strong ($M_1 > 2$) and very strong characteristics ($M_1 > 4$).

- The value of Re_2/Re_1 is approximately equal to 0.41 and 0.57 respectively for the CME20/11/2003 and CME11/04/2010 (Fig.1). These two results indicate that the upstream fluids have more turbulent character than the downstream fluid [34] for both CMEs.

- The κ values of shocks are 3.6 and 3.25 for CME20/11/2003 and CME11/04/2010 respectively.

- From Fig.4, the values of aftershock velocity are equal to 122 km/s and 115 km/s for the shocks after CME20/11/2003 and CME11/04/2010 respectively.

- With the use of the values of upstream Mach number 3.6 and 5, the values of sound speed in the interplanetary medium can be calculated as 103 km/s and 88 km/s for given values of u_1 in Table 1. They are in agreement with the estimates of [11] and [12]. Their estimation is about 90 - 100 km/s.

- For M_1 dependency $S_2 - S_1$ is increasing with increasing tendency of M_1. For very weak shocks of $M_1 < 1.2$ they become nearly isentropic [17] and [35]. For Re_2/Re_1 dependency of entropy difference, shock becomes isentropic for increasing values of Re_2/Re_1.

- $S_2 - S_1$ is increasing with greater values of κ. In other words, $S_2 - S_1$ has an increasing tendency for increasing values of downstream density.

- Similar to the density case, the downstream temperature has also increasing trend with the increasing values of $S_2 - S_1$.

- Unlike to κ and T_2/T_1 variations, $S_2 - S_1$ decreases with increasing values of u_2/u_1.

[1] Canakkale Onsekiz Mart University, Arts & Science Faculty, Physics Department 17100, Canakkale, Turkey, h_cavus@comu.edu.tr

[2] Canakkale Onsekiz Mart University, Graduate School of Natural and Applied Sciences, 17100, Canakkale, Turkey, goncazeybek@hotmail.com

ЭФФЕКТ ВЯЗКОСТИ В УДАРНЫХ ВОЛНАХ, НАБЛЮДЕННЫХ ПОСЛЕ ДВУХ РАЗЛИЧНЫХ КОРОНАЛЬНЫХ ИЗВЕРЖЕНИЙ МАСС CME20/11/2003 И CME11/04/2010

Х.КАВУС, Г.ЗЕЙБЕК

Корональные извержения масс являются главным результатом высокой активности Солнца. Такая активность способна генерировать в межпланетной среде ударные волны. Указанные волны возникают тогда, когда сверхзвуковые скорости солнечных частиц изменяются, становясь дозвуковыми. Поскольку действие вязкости на ударные волны является одной из центральных проблем в сверхзвуковом режиме течения сжимаемого газа, то изучение вышеуказанных явлений играет ключевую роль в задачах, связанных с космической погодой [1]. Основной целью данного исследования является изучение влияния вязкости на ударные волны, наблюденные после CME20/11/2003 и CME11/04/2010.

Ключевые слова: *ударные волны: вязкость: число Рейнольдса: корональное извержение масс*

REFERENCES

1. *J.Blazek*, Computational fluid dynamics: principles and applications, Elsevier, Amsterdam 2001.
2. *E.N.Parker*, Astrophys. J., **372**, 719, 1991.
3. *E.R.Priest*, Solar Magnetohydrodynamics, D.Reidel Publishing Company, Dordrecht, Holland 2000.
4. *S.K.Antiochos, C.R. De Vore, J.A.Klimchuk*, Astrophys. J., **510**, 485 1999.
5. *M.Stix*, The Sun, Springer Verlag, 1991.
6. *J.E.Borovsky, H.O.Funsten*, Journal of Geophysical Research, **108**, 13-1, 2003.
7. *P.A.Sturrock, J.R.Spreiter*, Journal of Geophysical Research, **70**, 5345, 1965.
8. *H.Cavus, D.Kazkapan*, New Astronomy, **25**, 89, 2013.
9. *A.P.Rouillard, D.Odstrcil, N.R.Sheeley et al.*, Astrophys. J., **735**, 7, 2011.
10. *T.Suzuki*, Mon. Not. Roy. Astron. Soc., **349**, 1227, 2004.
11. *V.M.Nakariakov, L.Ofman, T.D.Arber*, Astron. Astrophys., **353**, 741, 2000.
12. *T.V.Stepanova, A.G.Kosovichev*, Advances in Space Research, **9**, 1855, 2000.
13. *P.Riley, J.A.Linker, Z.Mikic, D.Odstrcil*, Advances in Space Research, **38**, 535, 2006.
14. *E.K.J.Kilpua, A.Isavnin, A.Vourlidas et al.*, Annales Geophysicae, **31**, 1251, 2013.
15. *M.Morduchow, P.A.Libby*, J. Aeron. Sci., **16**, 674, 1949.
16. *H.Hamad*, Zeitschrift für angewandte Mathematik und Physik, **49**, 827, 1998.
17. *H.Cavus, A.Kurt*, Astrophys. Bull., **70**, 220, 2015.
18. *H.Cavus*, Advances in Astronomy, (doi:10.1155/2013/58296), 2013.
19. *N.Gopalswamy, S.Yashiro, G.Michalek et al.*, Geophysical Research Letters, **32**, L12S09-L12S13, 2005.
20. *C.J.Davis, C.A. de Koning, J.A.Davies et al.*, Space Weather, **9**, S01005-S01020, 2011.
21. *H.Cavus*, Astrophys. Bull., **70**, 117, 2015.
22. *J.Vandegriff, K.Wagstaff, G.Ho, J.Plauger*, Advances in Space Research, **36**,

2323, 2003.

23. *O.Reynolds*, Philosophical Transactions of the Royal Society, **174**, 935, 1883.
24. *F.C.Bruhn*, *K.Pauly*, *V.Kaznov*, Proceedings of The 8th International Symposium on Artificial Intelligence, Robotics and Automation in Space (iSAIRAS), Munich-Germany, 2005.
25. *G.A.Gary*, Solar Physics, **203**, 71, 2001.
26. *W.H.Matthaeus*, *S.Ghosh*, *S.Oughton*, *D.A.Roberts*, Journal of Geophysical Research, **101**, 7619, 1996.
27. *J.A.Gonzales-Esparza*, *P.Corona-Romero*, *E.Aguilar-Rodriguez*, Proceedings of XXIX International Conference on Phenomena in Ionized Gases, Cancun-Mexico, 2009.
28. *D.Tsiklauri*, *V.M.Nakariakov*, *T.D.Arber*, Astron. Astrophys., **395**, 285, 2002.
29. *E.N.Parker*, Astrophys. J., **134**, 20, 1961.
30. *T.E.Holzer*, *W.I.Axford*, Ann. Rev. Astron. Astrophys., **8**, 31, 1970.
31. *M.V.Eselevich*, *V.G.Eselevich*, Astronomy Reports, **55**, 359, 2011.
32. *Y.B.Zel'dovich*, *Y.P.Raizer*, Physics of Shock Waves and High-Temperature Hydrodynamic Phenomena, Dover Publications Inc., New York, 2002.
33. *I.Veselovsky*, Astrophys. Space Sci., **277**, 219, 2001.
34. *Z.U.A.Warsi*, Fluid dynamics: Theoretical and Computational Approaches, Boca Raton Fla., CRC Press, 1999.
35. *H.Cavus*, Earth Moon Planets, doi:10.1007/s11038-016-9492-3, 2016.